Acta Medica et Biologica
Vol. 42, No. 2, 63-70, 1994

Scanning Electron Microscopic Study of Rat Ameloblasts during Enamel Maturation

Masaru KISHINO, Takeshi HAMADA and **Takao INOUÉ***

Department of Oral and Maxillofacial Surgery, and *Department of Anatomy, Faculty of Medicine, Tottori University, Yonago, Tottori 683, Japan

Received February 22, 1994

Summary. **The distal surface of rat incisor ameloblasts at the early stage of enamel maturation was investigated by high resolution scanning electron microscopy (SEM). Specimens were fixed by perfusion with 0.5% formaldehyde and 0.5% glutaraldehyde followed by decalcification, then freeze-cracked and treated with dilute osmium tetroxide to digest the dense lamina lining the distal surface of the ameloblasts. In this preparation, the unobscured distal surface was clearly demonstrated three-dimensionally under SEM. The following three types of ameloblasts were identified based on their ultrastructural features: ruffle-ended ameloblasts (RA); smooth-ended ameloblasts (SA); and transitional ameloblasts (Ruffle- to smooth-ended ameloblasts, R-SA). The surface of the RA was characterized by a complex labyrinth formed by protrusions and invaginations of the plasma membrane. In the RA and R-SA, microfibrils connecting the protrusions of the plasma membrane were observed on the distal surface. In these ameloblasts, small granules, presumably connecting the dense lamina to the distal surface of the ameloblasts, were also visible. The distal surface of SA was smooth, and no granular substances were visible on it. Mitochondria accumulated under the distal cell surface or the ruffle border. The surface structures of the R-SA displayed a pattern intermediate between those of the RA and SA. SA were distributed as several band-like structures at the stage of enamel maturation. These structural differences of the ameloblasts appeared closely related to enamel maturation.**

INTRODUCTION

The rat incisor is an excellent model system for studying amelogenesis.[1,2] Its distal surface in particular has received great attention from the viewpoint of enamel formation. The ameloblasts at the early stage of enamel maturation are classified into three different groups based on the morphological findings for the distal surface: ruffle-ended ameloblasts (RA), smooth-ended ameloblasts (SA) and transitional ameloblasts (TA) that show findings intermediate between those of RA and SA.[3] Josephsen and Fejerskov[4] further classified TA into two types: ruffle- to smooth- ended ameloblasts (R-SA) and smooth- to ruffle- ended ameloblasts (S-RA). Since these different types of ameloblasts are known to differ in calcium transport and endocytosis activities,[2] their ultrastructural study serves to clarify the mechanism of enamel mineralization. The ultrastructure of each has been studied by transmission electron microscopy (TEM).[4-7] Although several scanning electron microscopy (SEM) studies of ameloblasts have been available,[3,8-11] the distal surface at the stage of enamel maturation has not been clearly demonstrated because of the presence of a dense lamina lining this surface. In this study, we prepared specimens by the aldehyde-osmium-dimethyl sulfoxide-osmium (A-O-D-O) method in combination with the decalcification technique used in the preparation of bone tissues. As a result, the dense lamina was completely removed and the surface structures of the ameloblasts were clearly demonstrated. Furthermore, the intracellular structures were simultaneously demonstrated together with the surface morphology. In our preliminary report, we briefly introduced the morphology of the distal surface of ruffle-ended ameloblasts observed by SEM.[12] This paper describes in further detail the three-dimensional morphology of the distal surface of each type of ameloblast, and compares their morphological features.

MATERIALS AND METHODS

Specimens for preparation by the A-O-D-O method[13] were obtained from 3-week-old Wistar rats. After anesthetizing by intraperitoneal injection of Nembutal, a mixture of 0.5% glutaraldehyde and 0.5% formaldehyde in 1/15 M phosphate buffer (pH 7.4) was perfused from the left ventricle. The lower incisors and adherent alveolar bone were dissected from the surrounding tissues. They were washed in the same buffer followed by decalcification with 0.3 M ethylenediamine tetraacetic acid for 5 days. They were then postfixed with 1% osmium tetroxide in the same buffer. After a washing in the buffer, they were immersed in 25% and 50% dimethyl sulfoxide (DMSO) for 60 min each. Each specimen was then frozen on a metal plate chilled with liquid nitrogen, and split into two pieces with a precooled razor blade and a hammer using a freeze-cracking apparatus (TF-2, Eiko Engineering Co. Ltd., Japan). The two split specimens were placed in 50% DMSO at room temperature and thawed. They were rinsed in the buffer and placed in 0.1% osmium tetroxide for 96 h to remove excess cytoplasmic matrices (the osmic maceration procedure in the A-O-D-O method). After conductive staining with 2% tannic acid and 1% osmium tetroxide,[14] they were dehydrated through a graded ethanol series and finally dried with t-butyl alcohol.[15] The dried specimens were glued onto a specimen stub, coated with platinum to a thickness of approximately 3 nm with an ion-sputter coater (VX-10R, Eiko Engineering Co. Ltd., Japan), and observed with a field emission SEM (HFS-2ST, Hitachi Ltd., Japan) at 25 kV.

RESULTS

Since the maceration procedure employing dilute osmic solution is a delicate technique, the dense lamina lining the distal surface may remain undissolved, prohibiting the demonstration of the true distal surface of the ameloblasts. However, when the osmic maceration was carried out as intended, the dense lamina was completely dissolved. Although the distal surface was originally closely associated via the enamel with the dense lamina, a viewing space was created due to the dissolution of the lamina together with the artifactous shrinkage of the ameloblasts during specimen preparation. Consequently, the distal surface was successfully demonstrated under SEM (Fig. 1a). Furthermore, the intracellular structures were three-dimensionally demonstrated on the fractured surface.

Since an SEM image has a deep focal length, both

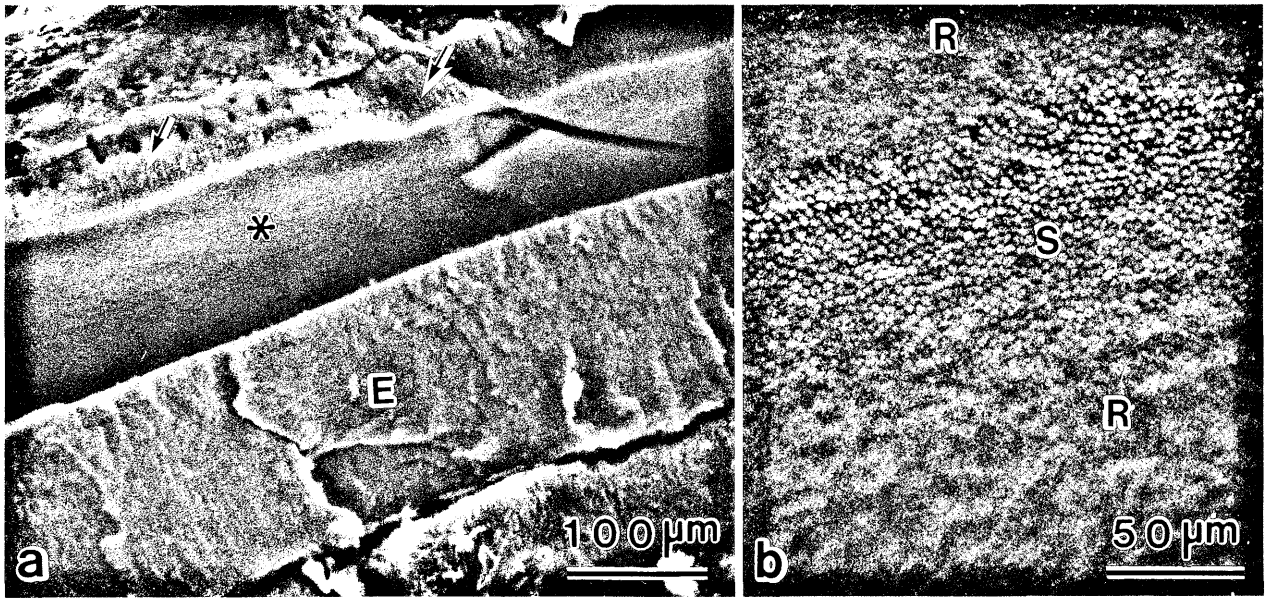

Fig. 1. a: A low-magnification micrograph of the fractured surface of a rat lower incisor, demonstrating a layer of ameloblasts (arrows) and decalcified enamel (*E*). The asterisk indicates the distal surface of ameloblasts. **b:** Higher magnification micrograph of the distal surface. The smooth-(*S*) and ruffle-(*R*) ended ameloblasts are arranged in bands.

the distal surface and intracellular structures could be simultaneously observed. The three types of ameloblasts (RA, SA and TA) at the early stage of enamel maturation were easily identified at high magnification based on their distal surface morphology. At low magnification, hexagonal cell contours were evident in the distal surface of the SA, but were less distinct in the RA. The SA and RA were arranged in alternating bands, and the TA was located between the SA and RA (Fig. 1b). The measured width of the SA bands was 150-250 μm. Since the border between the TA and RA bands was not clearly defined, measurement of the individual ameloblasts was difficult. However, the total measured width of each band comprising SA and RA was approximately 500-1000 μm.

Ruffle-ended ameloblasts (RA)

The RA were characterized by the presence of a ruffled border at their distal end (Fig. 2a, b). At low magnification, the cell boundary of the ameloblasts was unclearly defined (Fig. 2c). At high magnification, however, the ruffled border at the distal surface of the RA was seen. The surface was highly interdigitated, forming a complex labyrinth comprising protruded and invaginated plasma membranes. The fractured surfaces of the labyrinth was well visualized at higher magnification. The protrusions measured 0.1-0.2 μm in width and formed interdigitations. At higher magnification, the distal cell surface showed two types of minute granules, i.e., small and large granules measuring 10-20 nm and 70 nm diameter, respectively (Fig. 2d). The former were more numerous than the latter. Another characteristic of the distal surface of the RA was the presence of microfibrils connecting the protrusions of the plasma membrane. The microfibrils on the specimens with the 3-nm coating of platinum measured 7 nm in width.

The simultaneous observation of the distal free surface and fractured surface enabled the three-dimensional visualization of the ultrastructures concerned. An accumulation of mitochondria was evident under the ruffled border. Vesicular structures measuring 0.5 μm in diameter were interposed between the ruffled border and the mitochondrial accumulation.

Smooth-ended ameloblasts (SA)

The SA were characterized by their smooth cell surface without invaginations (Fig. 3a, b). On the distal surface free from the dense lamina, the cell boundaries bulged slighly toward enamel, showing hexagonal patterns when viewed from the top (Fig. 3c). The width of the hexagonal pattern, which was corresponded to the width of the SA, was approximately 5 μm. The surface was dotted with minute round or oval depressions measuring 0.1-0.3 μm in diameter. At low magnification, these appeared to be the openings of pinocytotic vesicles; they were not due to pinocytotic activity, however, because they were irregular in shape when viewed at high magnification (Fig. 3d). Granular structures such as those observed on the distal surface of the RA were not recognized on the SA.

On the fractured surface, the distal cell membrane was flat, and failed to form a ruffled border like that observed in the RA. A large accumulation of mitochondria was observed in the vicinity of the distal surface. Small vesicular structures measuring 100-200 nm in diameter were often observed under the surface cell membrane.

Ruffle- to smooth-ended ameloblasts (R-SA) in transitional ameloblasts (TA)

The ultrastructure of the TA displayed a pattern intermediate between those of the SA and RA. Although S-RA and R-SA are known in TA,[4] the former was poorly developed. Accordingly, this paper only describes the results on the ultrastructural features of the R-SA. On the fractured surface, slight invagination of the distal cell membrane was observed (Fig. 4a, b). Although at low magnification the cell boundaries were less distinct than those of SA, pits and clefts were observed on the distal cell surface (Fig. 4c). The clefts were randomly oriented. At higher magnification, the invaginations of the distal surface were not as highly developed as those seen in the RA. The invaginated distal cell membrane appeared to be fused with each other (Fig. 4d), although the smooth distal cell membrane may have separated, forming the invaginations of the RA. Microfibrils were present between the invaginations, as was noted in the RA, and the granular structures seen in the RA were also recognizable in the TA. Mitochondrial accumulation was evident under the invaginated distal cell membrane.

DISCUSSION

Previous TEM studies have revealed that the distal plasma membrane of ameloblasts, which is easily discerned in demineralized specimens, is in close

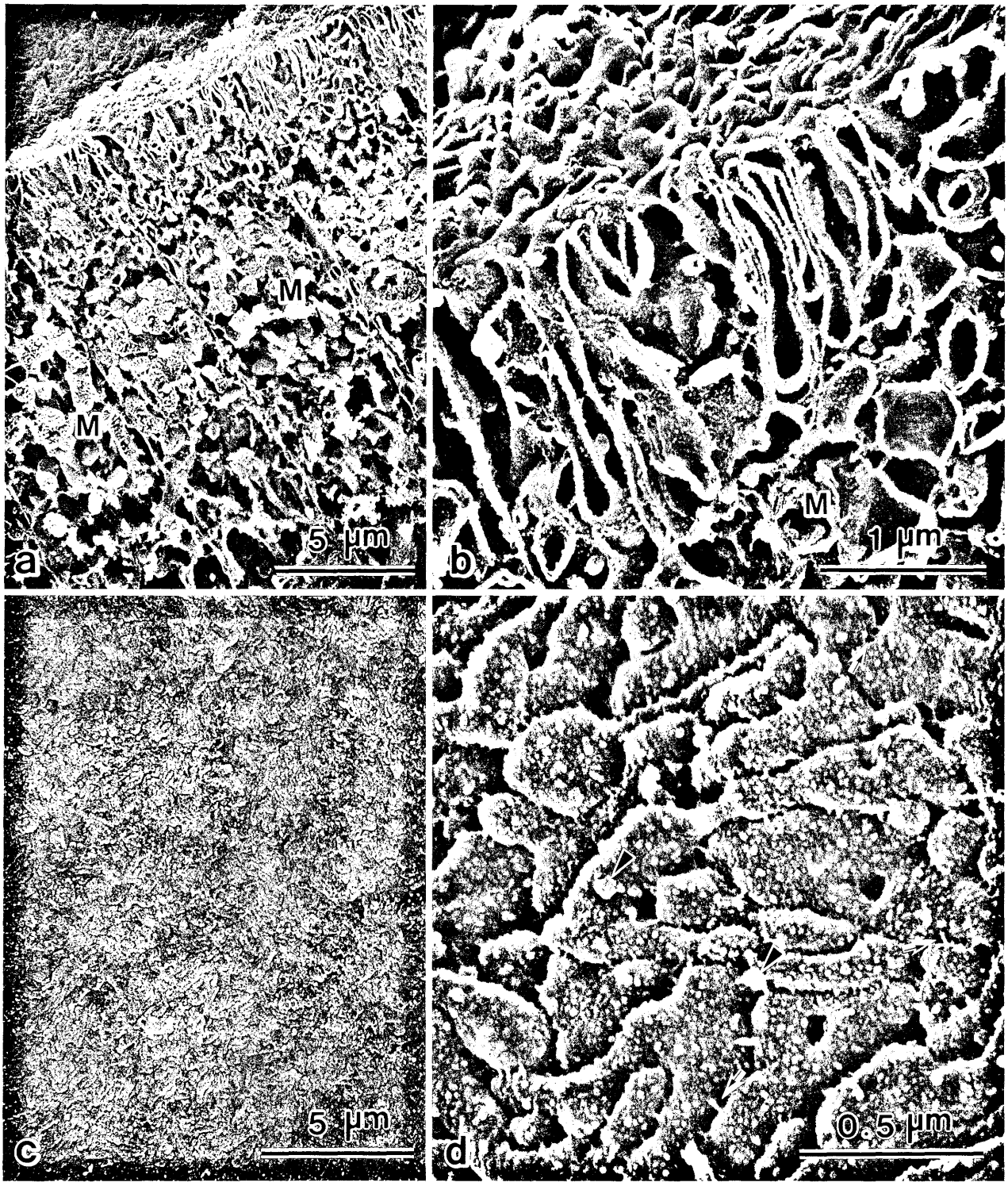

Fig. 2. Low (**a, c**) and high (**b, d**) magnification micrographs of ruffle-ended ameloblasts, showing the distal surface (**c, d**) and intracellular structures (**a, b**). A complex labyrinth comprising protrusions and invaginations of the plasma membranes can be clearly observed on the distal surface (**d**). The distal surface is dotted with many small granules and few larger granules (arrowheads). Note microfibrils connecting the protrusions of the plasma membrane (arrows). High magnification micrograph of the fractured surface shows the accumulation of mitochondria under the ruffle (**a**). *M*: Mitochondria.

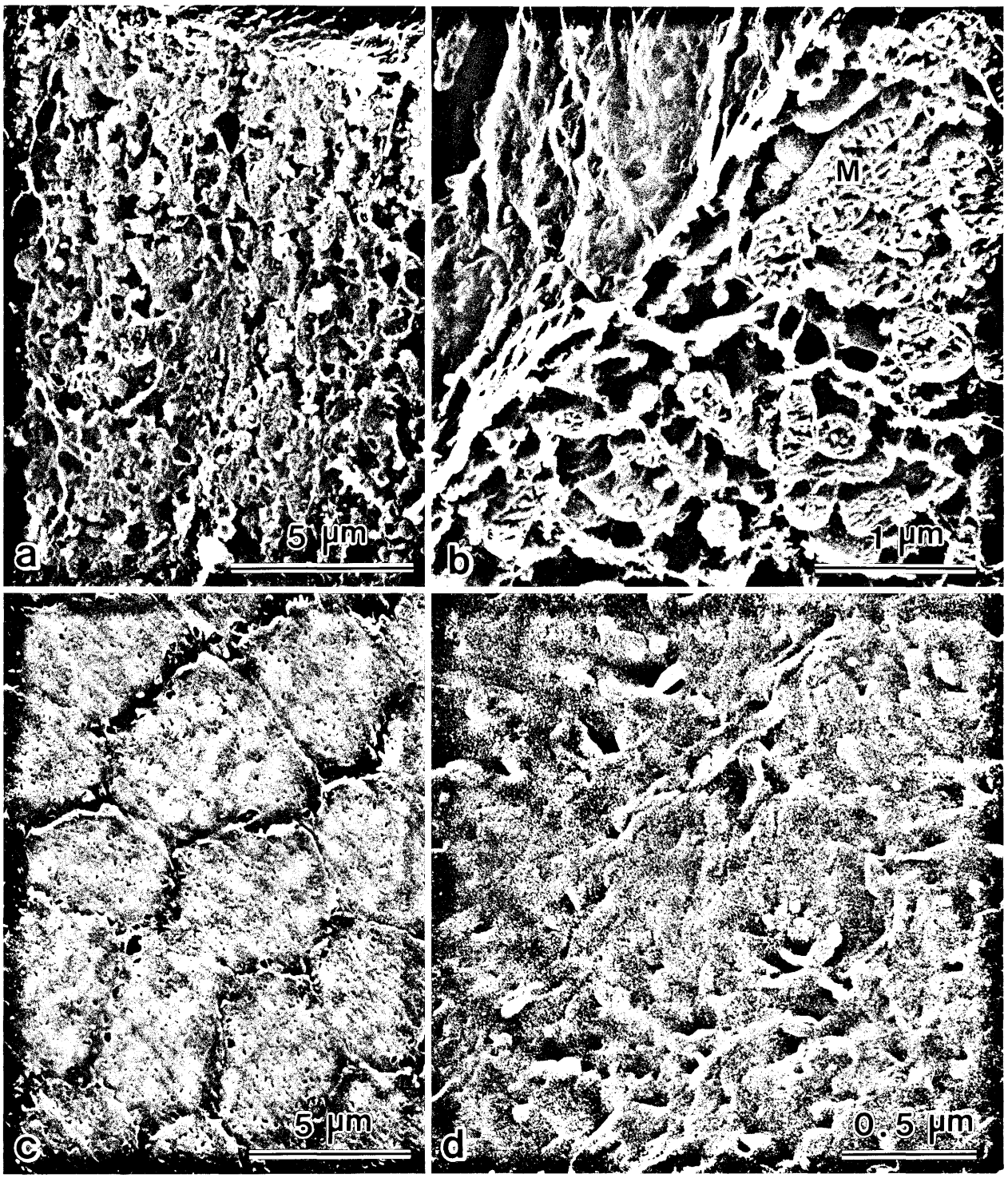

Fig. 3. Low (**a, c**) and high (**b, d**) magnification micrographs of smooth-ended ameloblasts, showing the distal surface (**c, d**) and intracellular structures (**a, b**). The distal surface is almost flat except for minute round or oval depressions (**d**). The accumulation of mitochondria (*M*) is seen in the vicinity of the distal surface (**b**).

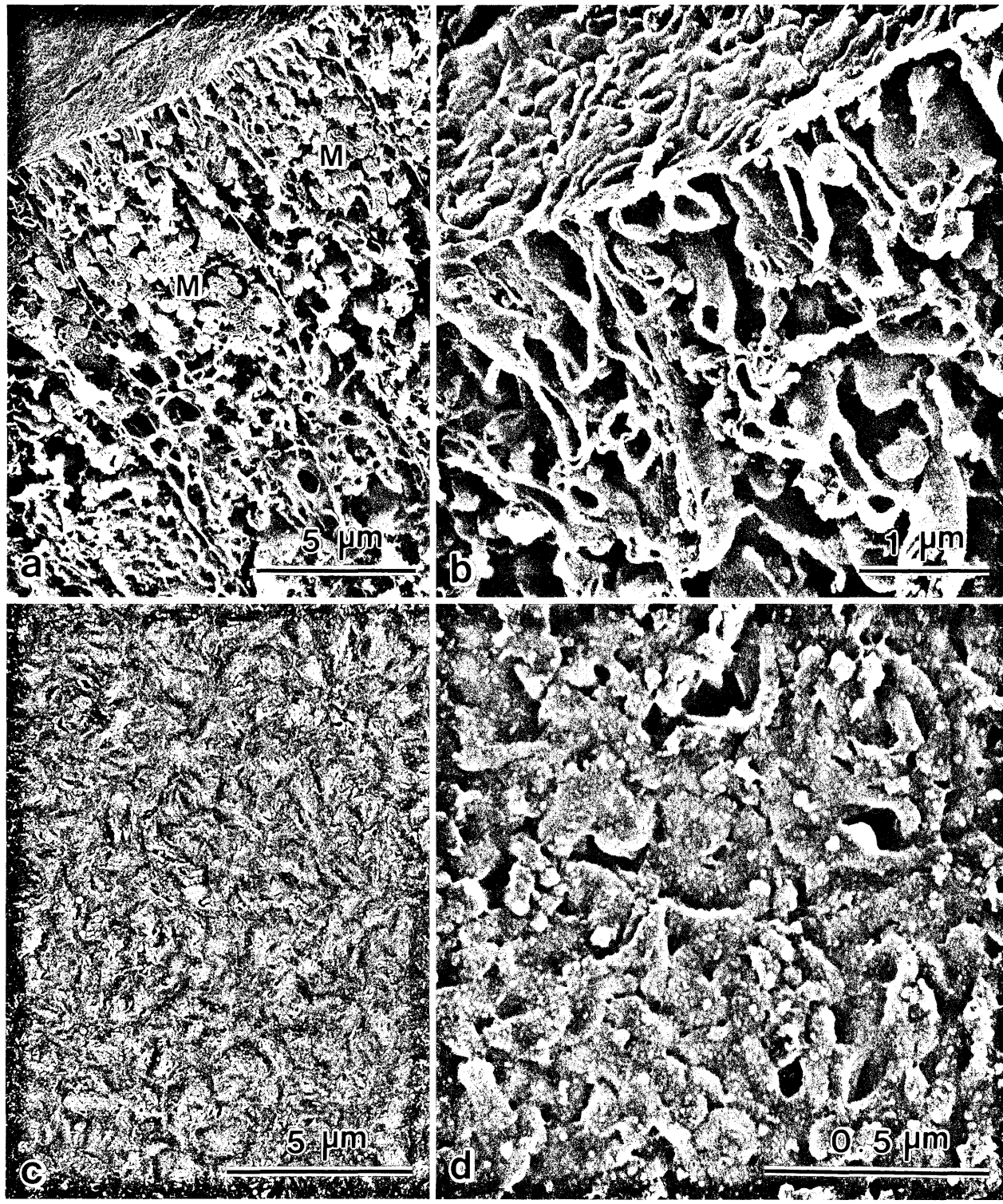

Fig. 4. Low (**a, c**) and high (**b, d**) magnification micrographs of transitional ameloblasts, showing the distal surface (**c, d**) and intracellular structures (**a, b**). On the fractured surface, a moderately developed brush border is visible (**b**). Arrows indicate microfibrils. *M*: Mitochondria.

apposition to a dense lamina.[4,6] As pointed out by Skobe,[8] it has been difficult to observe the distal surface of ameloblasts by SEM due to the presence of the lamina. The present specimen preparation technique, however, enables the direct observation of the distal surface once the dense lamina is dissolved during the osmic maceration procedure. Several authors have reported that this dense lamina is similar to the basal lamina recognized between epithelial cells and underlying connective tissues.[4,6] However, typical basal lamina remains intact after the osmic maceration procedure.[16] Furthermore, the microfibrils of the basal lamina are finer than those of the dense lamina.[12]

Cyclic changes of ameloblasts are well known to occur during amelogenesis; the shape of the RA changes to that of SA and subsequently to that of RA again. As shown even at low magnification (Fig. 1b), the distal surface are quite different between the RA and SA. The low magnified micrograph obtained in this study is quite identical to that reported by Takano.[17] The structure of TA is intermediate between those of RA and SA, which are arranged in periodical bands oriented transversely or at an oblique angle to the long axis of the tooth in the rat incisor.[2,18,19] During the maturation stage, ameloblasts in the mandibular incisor show a rapid modulation between ruffled- and smooth-ended structures in a short period.[20] Josephsen and Fejerskov[4] classified TA into two types: S-RA and R-SA. According to their study, the transitional zone of S-RA was developed within a distance of one or two cell, whereas that of R-SA was 75–100 μm wide. We only describe the ultrastructure of R-SA, but the comparison between R-SA and S-RA by SEM would be important for understanding the change of the distal plasma membrane during amelogenesis.

The present SEM study demonstarted a complex labyrinth on the distal surface in RA, which could not be readily apprehended by examining the two-dimensional TEM images. Two types of minute granules were visible on the distal surface of the RA and TA (R-SA), but not the SA. In a preliminary study, we speculated that the smaller granules were an inherent structure which anchors the dense lamina to the distal surface of the ameloblast,[21] because they resemble the granular substances found on the basal cell membrane facing the basal lamina of mesothelial cells.[16] Josephsen and Fejerskov[4] reported membrane-bound granules about 40–60 nm in diameter located between the dense lamina and distal cell membrane in the areas containing SA and RA. The reported size of these granules is similar to that of the large granules we observed in the RA and TA (R-SA), however, their significance is unknown. The lack of granular structures on the distal surface of the SA suggests that the distal surface of the SA is unconnected to the dense lamina.

Microfibrils connecting the protrusions of the labyrinth were observed only in the RA and TA (R-SA). These microfibrils may be derived from the dense lamina and play a role in packing the ruffled border.

Another finding obtained by SEM was the hexagonal pattern of the cell boundaries in SA when observed on the distal surface. Since the distribution of the SA is narrower than that of the RA, it is generally difficult to identify the SA on a fractured surface. The present method of simultaneous observation of intra- and extra-cellular structures seems to be quite useful in clarifying the ultrastructure during cyclic changes in amelogenesis.

REFERENCES

1) Reith EJ: The ultrastructure of ameloblasts from the growing end of rat incisors. *Arch Oral Biol* **2**: 253–262, 1960.
2) Takano Y, Ozawa H: Ultrastructural and cytochemical observations on the alternating morphologic changes of the ameloblasts at the stage of enamel maturation. *Arch Histol Jap* **43**: 385–399, 1980.
3) Sasaki T, Debari K, Higashi S: Peroxidase-distribution pattern in rat maturation-ameloblast layer, as revealed by high-resolution scanning electron microscopy. *J Electron Microsc* **33**: 168–171, 1984.
4) Josephsen K, Fejerskov O: Ameloblast modulation in the maturation zone of the rat incisor enamel organ. A light and electron microscopic study. *J Anat* **124**: 45–70, 1977.
5) Reith EJ: The stages of amelogenesis as observed in molar teeth of young rats. *J Ultrastruct Res* **30**: 111–151, 1970.
6) Warshawsky H: A light and electron microscopic study of the nearly mature enamel of rat incisors. *Anat Rec* **169**: 559–584, 1971.
7) Warshawsky H, Josephsen K, Thylstrup A, Fejerskov O: The development of enamel structure in rat incisors as compared to the teeth of monkey and man. *Anat Rec* **200**: 371–399, 1981.
8) Skobe Z: The secretory stage of amelogenesis in rat mandibular incisor teeth observed by scanning electron microscopy. *Calcif Tiss Res* **21**: 83–103, 1976.
9) Boyde A, Reith EJ: Scanning electron microscopy of rat maturation ameloblasts. *Cell Tiss Res* **178**: 221–228, 1977.
10) Skobe Z: Scanning electron microscopy of the mouse incisor enamel organ in transition between secretory and maturation stages of amelogenesis.

Arch Oral Biol **25**: 395-401, 1980.
11) Ohmi S: Three dimensional observations of the tubulo-vesicular system in the distal portion of ameloblasts. *Jap J Oral Biol* **29**: 332-362, 1987. (in Japanese with English abstract)
12) Kishino M, Ogawa T, Inoué T, Hamada T: Distal surface of the rat ruffle-ended ameloblasts at the stage of enamel maturation observed by scanning electron microscopy. *J Electron Microsc* **38**: 394-398, 1989.
13) Tanaka K, Mitsushima A: A preparation method for observing intracellular structures by scanning electron microscopy. *J Microsc* **133**: 213-222, 1984.
14) Murakami T: A revised tannin-osmium method for non-coated scanning electron microscope specimens. *Arch Histol Jap* **36**: 189-193, 1974.
15) Inoué T, Osatake H: A new drying method of biological specimens for scanning electron microscopy: The t-butyl alcohol freeze-drying method. *Arch Histol Cytol* **51**: 53-59, 1988.
16) Inoué T, Osatake H: Three-dimensional demonstration of the intracellular structures of mouse mesothelial cells by scanning electron microscopy. *J Submicrosc Cytol Pathol* **21**: 215-227, 1989.
17) Takano Y: Morphological and functional changes of the maturation ameloblasts of the rat incisor. In: Suga S (ed) Quintessence—Tooth enamel, its formation, structure, composition and evolution. Quintessence Pub. Co., Tokyo 1987, p 92-106. (in Japanese).
18) Reith E, Boyde A: The arrangement of ameloblasts on the surface of maturing enamel of the rat incisor tooth. *J Anat* **133**: 381-388, 1981.
19) Nanci A, Slavkin HC, Smith CE: Immunocytochemical and radioautographic evidence for secretion and intracellular degradation of enamel proteins by ameloblasts during the maturation stage of amelogenesis in rat incisors. *Anat Rec* **217**: 107-123, 1987.
20) Smith CE, McKee MD, Nanci A: Cyclic induction and rapid movement of sequential waves of new smooth-ended ameloblast modulation bands in rat incisors as visualized by polychrome fluorescent labeling and GBHA-staining of maturing enamel. *Adv Dent Res* **1**: 162-175, 1987.
21) Kishino M, Ogawa T, Hamada T, Inoué T: Ultrastructure of rat ameloblasts during enamel maturation observed by scanning electron microscopy. In: Suga S, Nakahara H (eds) Mechanisms and phylogeny of mineralization in biological systems, Springer, Tokyo 1991, p 211-215.